Light Metals 2015
Edited by: Margaret Hyland
TMS (The Minerals, Metals & Materials Society), 2015

Light Metals 2015

ELECTRODE TECHNOLOGY FOR ALUMINUM PRODUCTION

Anode Properties

SESSION CHAIR
Mario Fafard
Laval University
Quebec, Canada

Houshang Alamdari
Laval University
Quebec, Canada

Light Metals 2015
Edited by: Margaret Hyland
TMS (The Minerals, Metals & Materials Society), 2015

Evaluating the Crack Resistance of Carbon Anodes: Implementation of a Measurement System for Tensile Strength and Fracture Toughness

Dag Herman Andersen and Hogne Linga
Hydro Aluminium, Primary Metal Technology; Årdalstangen, 6885, Norway

Keywords: carbon anode, fracture, measurements, tensile strength, fracture toughness, laboratory

Abstract

Monitoring anode mechanical strength is increasingly important in production and operation of carbon anodes in high amperage cells due to higher crack driving forces. To achieve a better understanding of the directional crack resistance of the anode, a laboratory testing rig has been developed and installed at Hydro Aluminium Primary Metal Technology. The rig consists of a high-precision testing machine and a Hydro-developed measurement system which calculates the Young's modulus of elasticity, the tensile strength, the fracture strain and the fracture toughness. The equations of the physical parameters are derived from a finite element modelling of the specimen loadings, and are implemented in a Hydro developed laboratory software which computes the values from load-deflection data and transfers the parameters to a database. The paper outlines this method including the sample preparation machine.

Introduction

In Hydro experience, the traditional laboratory routine measurement of compressive strength and Young's modulus (YM) does not alone correlate to the cracking frequency of the anodes, neither in cell operations nor in the anode manufacturing processes. It was therefore a need to establish a measurement system to monitor the crack resistant properties like tensile strength and fracture toughness. These parameters were expected to give important information about how the quality of the anode material could be improved as regards choice of raw materials, the particle size distribution of the aggregate, and settings in the mixing-, forming- and baking-processes. The information could also be used in anode design and for different process adjustments, for instance by targeting a maximum level of the crack driving forces to not exceed the measured anode fracture toughness.

The Flattened Brazilian Disk (FBD) test or splitting tension test, which is performed by compression with diametrically opposite concentrated loads on a disc specimen, was implemented. The reason for choosing this method was mainly the possibility to extract several material parameters from one loading test, including tensile strength, fracture toughness, YM and fracture strain [1][1]. Secondly, this test makes it possible to use a simple specimen design in order to keep sample preparation costs at a low level. A drawback is that there exist no exact analytical equations of the four parameters with the "flattening design", only for point loading design. But approximate equations have been derived [1-3] for other material types and dimensions in publications from mining and rock science. A set of equations were therefore developed by Hydro for the carbon anode materials, by finite element modelling (FEM) of the loading test using the measured load-deflection data as input in the developed equations. These equations were verified and shown to be consistent with the equations in the other publications [1-3]. An important consideration is the choice of a larger diameter of the disk specimen. This improves the probability of determining the fracture toughness which demands a finite crack length (after maximum load is achieved) and which will not be measurable if the specimen divides into two parts at once. The larger dimensions also increase the possibility for better correlations with the anode manufacturing parameters, since the specimen dimensions will be several times higher than the maximum coke particle in the material.

Other factors were also considered, including material anisotropy. Reference [4] reported tensile strength and toughness values 10 % higher in the horizontal anode plane compared with the vertical anode plane. The developed equations of the four material parameters were therefore made directional; one set of equations for vertical loading and another set of equations for horizontal loading of the anode material.[2]

The equations were then hardcoded into the developed software, named StressLink[3], which has a user friendly graphical interface for laboratory use. StressLink imports the measured load-deflection curve from the loading test and extracts the four parameters from the data set by using the equations derived by FEM. The material parameters are then transferred to a local database for later processing or transfer in the Hydro intranet.

Sample preparation

The sample preparation machine shown in Figure 2 is transforming a solid carbon cylinder into the three disks shown in Figure 1 in two operations; first the cylinder is slit (by sawing) to make the flattened surfaces for the contact force in the load-deflection test; secondly the cylinder is cut into three discs.

The flattened disks are axis symmetric. The rotation, movement and the load on the saw blades are controlled by a PLC and the set points are reachable from a panel of electric potentiometers. The machine and PLC conforms to the machine directive[4]. The construction, engineering and installation were done in

[1] These are denoted "the four parameters" in this publication.

[2] In the FEM model, the anode was regarded as a linear transversal isotropic material.

[3] StressLink is a .net software application developed by Hydro Aluminium - Primary Metal Technology.

[4] The sample preparation machine is CE marked in accordance to F20.05.2009 nr. 544, 2006/42/EC, 2006/95/CE and 2004/108/EC

cooperation between Hydro Aluminium - Primary Metal Technology (PMT) in Årdal and HMR[5].

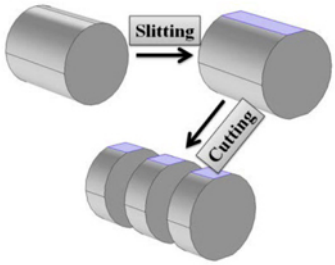

Figure 1: A solid cylinder of carbon material is changed to three FBD specimens in the sample preparation machine in a two stage operation of slitting and cutting by sawing.

The sawing blades in the machine are fixed to the rotating cam. The geometry is flexible - if the specimens in the future are changed a new set of cam and blades can be mounted.

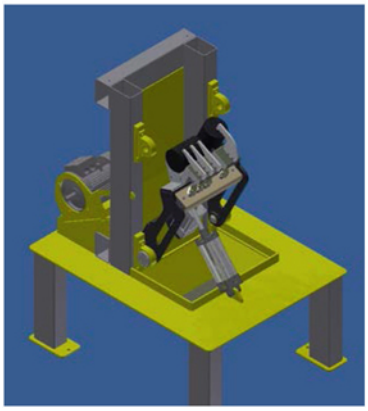

Figure 2: The sample preparation machine for making the FBD specimens. The machine is built into and completely covered in a safety box with outlet for suction of carbon dust.

Measurement of the load-deflection curve

A 100 kN-loading machine from Zwick[6] was configured for the FBD test rig shown in Figure 3. The machine is controlled by the software, testExpert, which is a product from Zwick. The *load-vertical deflection*-curve (without extensometer) and the *load-horizontal deflection*-curve (with extensometer) are both recorded. It should be noted that the four parameters are all derived from the *load-vertical deflection*-curve. The horizontal deflection, measured by the extensometer, is today only used to verify the FE-modelling and the resulting equations of the four material parameters. Additionally the horizontal deflection can be used to measure the Poisson-ratio of the material. The model work showed that the horizontal measurement can be used to find some of the material parameters for two material directions in one loading test. But in such a case, the equations will be dependent of the horizontal extensometer and this will increase the risk of inaccuracy since the horizontal deflection is much less than the vertical deflection during the loading process. Even though such a possibility exists, the equations of the four parameters presented in the next section are based upon making one loading test for each directional set of the material parameters so the equations in this publication are therefore chosen not to be dependent of the horizontal extensometer.

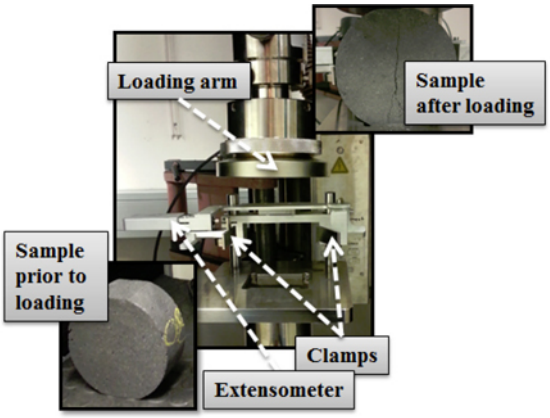

Figure 3:A FBD (left photo) is set into the Zwick test rig between the clamps of the horizontal extensometer. The loading arm is displacement controlled downward and a vertical crack is generated (upper right photo) due to the tensile stresses set up in the horizontal direction.

This means that two loading tests must be performed for calculating material parameters of two material directions. A typical *load-vertical deflection*-curve (*F-w*-curve) is shown in Figure 4 including which part of the curve is used to calculate which material parameter.

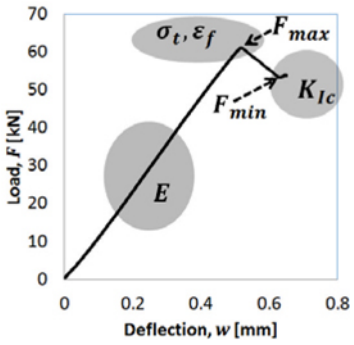

Figure 4: A measured load-deflection-curve (*F-w*-curve) of a carbon specimen by the FBD test (deflection in the same direction as the loading force). The material parameters are found from different parts of the curve.

The loading test is stopped after a minimum force, F_{min} is detected. The minimum force is used to calculate the fracture toughness by the Stress Intensity parameter Mode I, K_{Ic}, which is a toughness property from linear elastic fracture mechanics. The linear part of the *F-w*-curve is used to calculate Young's modulus. The maximum load, F_{max}, and the corresponding deflection are used to estimate the tensile strength, σ_t, and the fracture strain, ε_f. The tensile strength, σ_t, is a measure of how resistant the material is to a breakage by tensile stresses, while the fracture toughness (K_{Ic} from F_{min}) is a measure of how resistant the material is against further expansion of an existing crack, created in F_{max}.
In Figure 5 the photos illustrate that there is a clear difference of the visually observed crack for a specimen with a high F_{min} (high toughness) compared by a specimen with a low F_{min} (low

[5] HMR Hydeq AS, mechanical company in Årdal, Norway.
[6] Zwick Gmbh, producer of material testing machines.

toughness). The crack is hardly visible for specimens with a high F_{min} (Sample A) but those specimens with a low F_{min} (Sample B) have a large crack which almost divides the specimens in two parts.

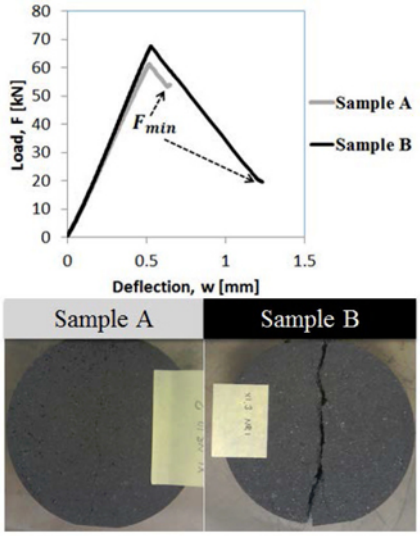

Figure 5: The cracks observed in loading tests with low F_{min}-values, like Sample B, are more uncontrolled and damaging than for loading tests measured with high F_{min}-values, like Sample A.

Interestingly, for some specimens measured with a low F_{min} it was observed a higher F_{max}, which means a higher tensile strength for sample B than for sample A. This indicates how important it is to include the fracture toughness into an anode measurement program since it will give information about how and when an anode will suffer serious and damaging crack extensions. This information would have been lost if only the maximum strength had been measured, and the wrong conclusion of sample B as the "best" could have been taken.

Finite Element Models of the specimen loadings

The equations of the four parameters are found by finite element modelling (FEM) and multiple regressions (MR) analysis of the numerical data from the models. The material in the model is a transversal isotropic material defined by a parallel (transversal) anode direction and a normal (horizontal) anode direction (isotropic plane). The four parameters, load and deflection (defined in the above section) are denoted $E^{\parallel}$, $\sigma_t^{\parallel}$, $\varepsilon_f^{\parallel}$, $K_{Ic}^{\parallel}$, $F^{\parallel}$, $w^{\parallel}$ when they are found by parallel loading of the specimen (loadings of the of the anode material which is parallel with the vibration direction of the anode in the vibrocompactor). In normal loading tests of the specimen (normal to vibration direction) the parameters are denoted $E^{\perp}$, $\sigma_t^{\perp}$, $\varepsilon_f^{\perp}$, $K_{Ic}^{\perp}$, $F^{\perp}$, $w^{\perp}$. For a transversal isotropic material there are two independent Poisson ratios, $\eta^{\parallel}$ (in the vertical anode plane along anode length), and $\eta^{\perp}$ for the horizontal anode plane. According to reference [5] the dependent Poisson ratio, defined in the vertical anode plane along the anode width, is given by the expression, $\eta_3 = \eta^{\parallel}\frac{E^{\perp}}{E^{\parallel}}$. The Shear modulus of the material is also dependent and given as $G^{\perp} = \frac{E^{\perp}}{2(1+\eta^{\perp})}$ for the horizontal plane and $G^{\parallel} = \frac{E^{\parallel}}{2(1+\eta^{\parallel})}$ for the two other planes [6] in the developed FE-model. A 3D quart contact FE-model was developed in COMSOL[7] as shown in Figure 6 to find the equations of the Young's modulus, tensile strength and fracture strain ($E, \sigma_t, \varepsilon_f$) while a 2D half contact model with different crack geometries, shown in Figure 7, was built to derive the equations of the fracture toughness by the stress intensity factor, K_{Ic} . In both models the material was transverse isotropic. The mesh in the left plot of Figure 6 consists of 18.000 tetrahedral elements. The colored surface plot at right shows the vertical displacement, w, when a force, F, loads the specimen (a rainbow color table scheme is used where the red colors have the highest vertical displacements).

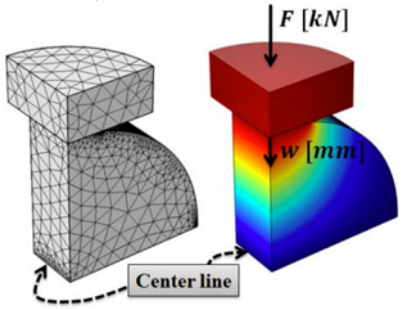

Figure 6: A force controlled 3D quart contact FE-model with a transverse isotropic material.

The value range of the 3D transverse isotropic material was modelled within the ranges, $E^{\parallel} = 4.5 - 9.5GPa$, $\frac{E^{\perp}}{E^{\parallel}} = 1 - 1.12$, $\eta^{\parallel} = 0.11 - 0.145$, $\frac{\eta^{\perp}}{\eta^{\parallel}} = 0.93 - 1.1$, with loading force up to $100\ kN$ (max. load of the Zwick Machine). A force controlled loading was defined in both models. As a contact pressure FEM technique the penalty method was chosen. For the 3D model a parametric sweep was set up by sweeping through 3840 numerical loading test combinations of $E^{\parallel}$, $\frac{E^{\perp}}{E^{\parallel}}$, $\eta^{\parallel}$, $\frac{\eta^{\perp}}{\eta^{\parallel}}$, F within the value ranges given above. The vertical deflection in the contact surface, w, and the maximum of the first principal stress and strain in the specimen's center line in Figure 6 was calculated by the model and exported to a file for each of the 3840 numerical loading tests. This gave a large data matrix which was analyzed by MR.

The 2D contact model in Figure 7 had a parameterized crack with a blunted circular crack tip of blunting radius, b, and a total crack length of $2a$. The arms load the flattening areas defined by the angle, α. The colored surface plot at right shows the first principal stress (SP1) and how this stress is concentrated at the crack tips when a certain load is applied from the loading arms. The horizontal deformation in the right plot is scaled up by $30x$. An integration path was set up around the upper crack tip in order to solve the J-integral. The number of triangular elements in the mesh in the left plot varied from 70.000 to 200.000 dependent of the crack geometry. The crack length was tested up to 90% of the specimen's diameter.

Linear elastic stress analysis of a sharp crack predicts infinite stresses at the crack tip. In real materials, however, stresses at the crack tip are finite due to inelastic material deformation. Since the 2D model is linear elastic it was decided to implement a blunted crack tip shape in order to study how the crack tip plasticity affects the equation of the fracture toughness. The value range of the 2D crack model was the same as for the 3D model, except that $E^{\parallel}$ was in the range from 4 to $7\ GPa$. The number of mesh points

[7] COMSOL Inc. provides software solutions for FE-modelling.

was constant in the blunted crack tip area regardless of the blunting, b, since the element size of the blunted circular shape was defined as $2\pi b/16$. This was to avoid secondary effects when the blunting radius was changed in the model. The model swept through 221 different crack geometries for 243 different materials within the material specification mentioned above. The lowest blunting factor tested in the model was at $b = 0.5\ \mu m$.
The equation proposed for the fracture toughness in the next section is exemplified when the 2D plane is chosen to be the vertical anode plane along the anode length.

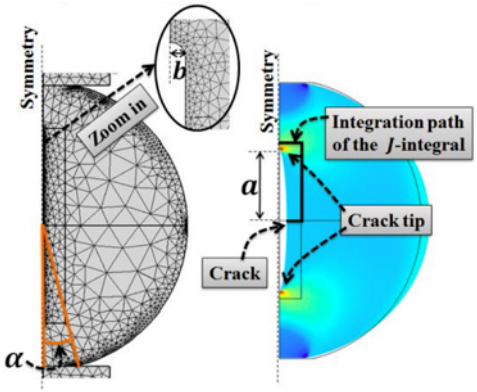

Figure 7: A 2D contact model with a parameterized crack (a and b) with a transverse isotropic material. The loading arms of steel are only shown in the left mesh plot.

Equations of the material parameters by regression analyses on the data from the finite element models

The post processed data from the FE-models, described in the above section, was exported to text files and studied by MR analysis to find equations (Equation 1, 3 and 7) which are valid within the ranges of the material parameters and the loading force used in the models. Since the material in the models is linear elastic, some of the equations will also be valid beyond these ranges. Note also that all the equations are given for a specific specimen dimension. The specimen dimensions are therefore not parameters in the equations.

The Young's modulus

The Young's modulus was found, as shown by Equation 1, for both loading directions, where $x =\parallel$ for parallel specimen loadings and $x = \perp$ for normal specimen loadings, normal to the vibrational anode direction. The coefficients, c_x, d_x , e_x , f_x, are constants from the MR analysis.

$$E^x = \left(c_x \frac{E^\perp}{E^\parallel} + d_x\right)\frac{F^x}{w} + e_x \frac{E^\perp}{E^\parallel} + f_x \qquad (1)$$

For normal loadings ($x = \perp$) it was found that Equation 1 could be simplified and still maintain the accuracy when $c_\perp = e_\perp = 0$, so that $E^\perp$ is completely dependent of the measured load-deflection slope, $\frac{F^\perp}{w}$, and not affected by the anisotropy term, $\frac{E^\perp}{E^\parallel}$, of the material. This is not the case for the parallel Young's modulus, $E^\parallel$, shown in the right plot of Figure 8, which also is dependent of the anisotropy term. The reason for the simplification of $E^\perp$ in Equation 1 is that the loading, $F^\perp$, is performed in the isotropic plane. In order to solve for $E^\parallel$, the anisotropy term must be known in addition to the measured load-deflection-slope, $\frac{F^\parallel}{w}$. For an isotropic material the term is $\frac{E^\perp}{E^\parallel} = 1$ but earlier anode measurements have shown that the term is up to 1.11 higher [4] for the anode material. Anode measurement programs can be performed in order to find a typical value of the anisotropy term. Equation 1 has a correlation better than $R^2 > 0.9994$ when comparing the Young's modulus from the 3D FE-model from the entire 3840 numerical specimen loadings described in the above section. The left plot of Figure 8 shows the correlation for normal loading tests by the FEM.

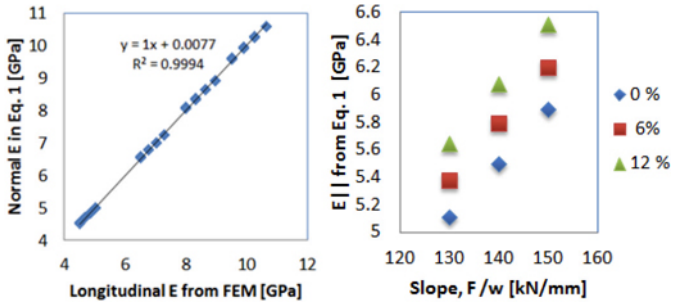

Figure 8: The left plot shows the normal Young's modulus, $E^\perp$, from Equation 1 plotted against $E^\perp$ from the 3D FE-model for all the normal loadings. In the right plot is $E^\parallel$ from Equation 1 plotted against F/w and the anisotropy terms, $\frac{E^\perp}{E^\parallel}$.

An equation of the Young's modulus for isotropic materials from the Rock Science Journal [1] is given in Equation 2, where t is the specimen thickness, η the isotropic Poisson ratio and α is the angle describing the extension of the flattened surface as shown in Figure 7. The equation from [1] was verified by an FE-model developed in ANSYS.

$$E = \frac{2F}{wt}\left\{(1-\eta) - ln\left(1 + \frac{4}{sin^2\alpha}\right)\right\}\frac{\alpha}{sin\alpha} \qquad (2)$$

It was found that Equation 1 (from our work) was calculating the Young's modulus not more than 2% lower than the ANSYS model in reference [1] which was used to verify Equation 2. Note that the ANSYS model is isotropic and also 2D while the COMSOL model in this work is transversal isotropic and in 3D. When comparing, the anisotropy terms are set to 1 ($\frac{E^\perp}{E^\parallel} = \frac{\eta^\perp}{\eta^\parallel} = 1$) in order to make our model isotropic.

The tensile strength

The maximum of the first principal tensile stress at the specimen's center line in Figure 6 is expressed in the proposed Equation 3 as the tensile strength when the measured load, F_{max}, is set into the equation (same directional notation as for Equation 1).

$$\sigma_t^x = (c_x\eta_\parallel + d_x)F_{max}^x + (e_x\eta_\parallel + f_x) \qquad (3)$$

The coefficients, c_x, d_x , e_x , f_x, are not constants but functions of the anisotropy ratio $r_E = \frac{E^\perp}{E^\parallel}$. Most of the coefficient functions are linear, but some coefficients are expressed by a second order polynomial (where r_E is the argument). For a material with a given r_E and $\eta_\parallel$ the tensile stress in the specimens centerline is completely proportional to the measured load, F. The stress from Equation 3 correlates to the first principal stress component, from the center line in the 3D model (Figure 6), with an accuracy of

$R^2 \geq 0.9999$ for all the numerical specimen loadings within the value ranges described in the above section, as shown for normal loadings in the left plot of Figure 9.

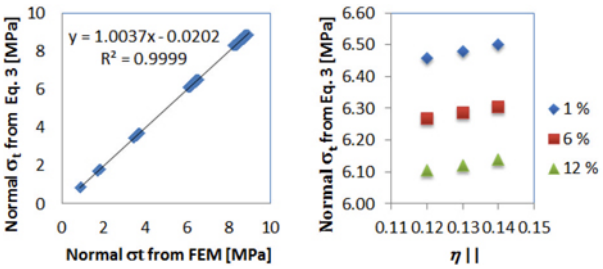

Figure 9: The left plot shows $\sigma_t^{\perp}$ from Equation 3 versus the first principal stress in the center line in the FE-model in Figure 6 for all the normal specimen loadings. In the right plot, Equation 3 is plotted versus $\eta_{\parallel}$ and $\frac{E^{\perp}}{E^{\parallel}}$ at a specific load, F_{max}.

Equation 3 from this work was also verified by the isotropic equation of the tensile strength in reference [1] given in Equation 4, where D is the specimen diameter, t the thickness and α is angle defining the contact surface area as shown in Figure 7.

$$\sigma_t = \frac{F_{max}}{\pi D t}\left\{\frac{\left(2cos^3\alpha + cos\alpha + sin\alpha/\alpha\right)^2}{8\left(cos\alpha + sin\alpha/\alpha\right)}\frac{\alpha}{sin\alpha}\right\} \qquad (4)$$

When comparing Equations 3 and 4, the anisotropy ratios, $\frac{E^{\perp}}{E^{\parallel}}, \frac{\eta^{\perp}}{\eta^{\parallel}}$, in Equation 3 are set to 1 in order to make Equation 3 isotropic. The strength values calculated in Equation 3 are not deviating more than 2% from the strengths calculated by Equation 4.

The fracture toughness

The fracture toughness, expressed by the stress intensity factor, K_{Ic}, for isotropic linear materials in a FBD test, is given by the following equation[1]:

$$K_{Ic} = \frac{\Phi_{max}}{t\sqrt{R}}F_{min} \qquad (5)$$

where R is the radius and t is the thickness of the specimen. The fracture toughness is proportional with the measured force minima, F_{min}, observed after specimen breakage (see Figure 4), since the dimensionless stress intensity factor, Φ_{max} is a constant for a given specimen dimension [1]. The force, F_{min}, corresponds to the point where crack stability is restored. As long as the force decreases drastically from the maximum force, F_{max}, the crack grows violently and fast. As long as the force, F, is decreasing during the unstable crack propagation, Φ must increase (because $K_{Ic} = constant$). However, when F_{min} is reached, the force must increase in order for further crack growth to occur. The dimensionless factor, Φ, will therefore reach a maximum, Φ_{max} at the measured force minima, F_{min}. By modelling, Wang[1] found the dimensionless factor, Φ, as a function of the crack length, a, and extracted the maxima from this curve (maxima of $\Phi(a)$). In our COMSOL model the J-integral (or J) [7] was used to find the toughness by K_{Ic} (see Figure 7). In order to transform the J-integral to K_{Ic}, equations by Liebowitz [8], which relate the different toughness factors in linear orthotropic materials, were used. When the material loading is assumed as a 2D plain strain model and the shear modules are given as described in the above section, the stress intensity factor is shown in Equation 6 for the presented 2D plane in the 2D model.

$$K_{Ic}^{x} = \sqrt{E^{\perp\prime}J_{Ic}^{x}} = \sqrt{\frac{\left(\sqrt{2E^{\perp}E^{\parallel}}\right)J_{Ic}^{\perp}}{\sqrt{\left(1-\eta^{\perp 2}\right)\left(1-\eta^{\parallel 2}\right)\left(1+\sqrt{r^x}\right)}}} \qquad (6)$$

The ratio r^x is for normal loadings given by $r^{\perp} = \frac{E^{\perp}}{E^{\parallel}}$ and for parallel loadings the ratio is $r^{\parallel} = \frac{E^{\parallel}}{E^{\perp}}$. The relation between the stress intensities from Equation 6 and the loading force of the specimen were studied in the model for different crack lengths in order to find Φ_{max} for each specimen tested in the model. The proposed Equation 7 was found by the MR study, and is valid within the material property ranges described in the above section by an acceptable accuracy of $R^2 > 0.992$ when plotting Equation 7 against the Φ_{max} from the FE-model for all the specimen loadings.

$$\Phi_{max}^{x} = \left(c^x\frac{E^{\perp}}{E^{\parallel}} + d^x\right)E^{x\left(e^x\frac{E^{\perp}}{E^{\parallel}}+f^x\right)} \qquad (7)$$

The equation is expressed with the same directional notation as used in Equation 1 and 3. The coefficients, c^x, d^x, e^x, f^x, were found by MR analysis (also for other 2D planes than the 2D plane presented in this publication). The toughness is found by setting Equation 7 into Equation 5. From the left plot in Figure 10, Φ_{max} for parallel specimen loadings is shown, where it decreases by a higher Young's modulus (elasticity in the same direction as the loading direction) and increases by the anisotropy ratio, $\frac{E^{\perp}}{E^{\parallel}}$. Equation 7 was verified by the model work of Keles [3] which uses an isotropic ABAQUS crack model to model andesite rock with a Young's modulus of $12.3\ GPa$. The right plot in Figure 10 shows how Equation 7 (when setting $\frac{E^{\perp}}{E^{\parallel}} = 1$ to make it isotropic) estimates almost the same Φ_{max} found for andesite rocks of $12.3\ GPa$ (Φ_{max} from Equation 7 at $E = 12.3GPa$ is 1.8% higher than Φ_{max} from [3]). The small deviation can be due to two factors; 1) the Young's modulus of $12.3\ GPa$ is not within the valid property range tested in our COMSOL model, and Equation 7 is thereby not valid for such extrapolation, 2) Equation 7, plotted in Figure 10, is shown when the blunting factor at the crack tip is $b = 0.5\ \mu m$. A small plasticity effect has therefore been included at the crack tip and the material will be tougher (higher Φ_{max}) against cracks than without crack blunting. Within the range of the blunting factors tested, Φ_{max} decreases approximately by 0.1% from $b = 1.5\ \mu m$ to $b = 0.5\ \mu m$. With linear extrapolation down to $b = 0$, indicating no plasticity in the crack tip, it is expected a toughness 0.04% lower at $b = 0$ compared with the toughness calculated at $b = 0.5\ \mu m$. Equation 7 set into Equation 5 gives typical toughness values of the anode material in the range of $K_{Ic} \approx 1.1 - 2.5\ MPa\sqrt{m}$ (dependent of raw material, recipe and other manufacturing conditions). This range of toughness is also consistent with toughness measurements of the anode material for other test methods, like the 3-point bending test described in [4]. The equations, 5-7, can also be used to find the established (isotropic) fracture energy [9] for anodes since the fracture energy is given by J in Equation 6.

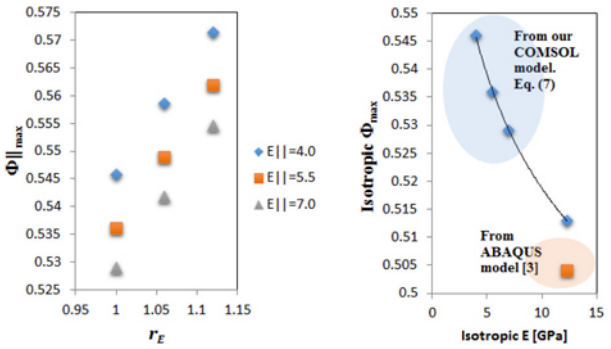

Figure 10: In the left plot, $\Phi_{\max}$ in Equation 7 for parallel specimen loadings increases by $r_E = \frac{E^{\perp}}{E^{\parallel}}$ and decreases by $E^{\parallel}$[GPa]. In the right plot, the isotropic part of Equation 7 is plotted versus the Young's modulus by setting $\frac{E^{\perp}}{E^{\parallel}} = 1$.

The fracture strain

In a linear material the strain is known by Hooke's law when the stress and the Young's modulus of the material are known. The non-linearity areas of the load-deflection curve in Figure 4 (in the beginning of the curve and at areas close to F_{max}) makes the real fracture strain higher than that calculated by Hooke's law. Since the 3D model is linear, the secant modulus (slope of line from 0 to F_{max}) is used as input in an equation found by MR analysis to calculate the fracture strain. The equation is not presented in this paper since the non-linearity of the load deflection curve mostly affects this parameter and the parameter will therefore have the largest uncertainty. The parameter is still recorded in the measurement program of anode materials.

Implementation of the equations into a laboratory software

A software application has been developed for the laboratory which contains all the material equations described in the above section. Parts of the graphical user interface of the software are shown in Figure 10.

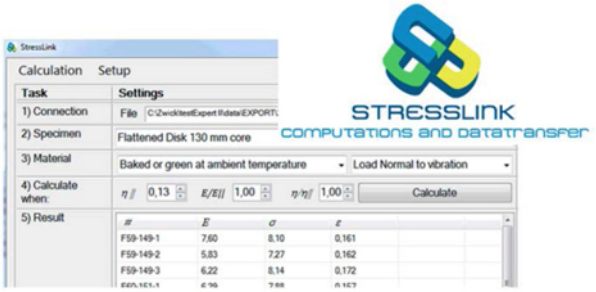

Figure 11: A part of the graphical user interface of the software, StressLink.

The Young's modulus $[GPa]$, tensile strength $[MPa]$ and fracture strain [%] for normal loading is calculated and placed into a table in this example. Each row in the table is a specimen with unique identification. The user first connects and uploads load-deflection data from a file generated by the testing machine. The user then specifies the specimen, material and loading types. Prior to calculation the user can specify the anisotropy ratio of the material if no sample tests in different directions have been performed.[8] After calculation the material parameters are transferred to a database.

Conclusion

The Flattened Brazilian Disk method has been implemented on a $100\,kN$ Zwick machine for load testing to determine anode mechanical properties where the discs are formed by a sample preparation machine developed for this test. Transverse isotropic equations for the tensile strength, fracture toughness by the stress intensity factor and the fracture energy Mode I, and Young's modulus have been derived and presented. The equations have been verified with other publications within rock science and found to be consistent. The isotropic part of the equations deviates not more than 2% from the referred results. The equations were found by FE-modelling and implemented into developed user friendly laboratory software.

Acknowledgements

The authors are thankful for the financial support from the Norwegian Research Council.

References

[1] Q. Z. Wang, X. M. Jia, S. Q. Kou, Z. X. Zhang, P. A. Lindqvist: "*The flattened Brazilian disc specimen used for testing elastic modulus, tensile strength and fracture toughness of brittle rocks: analytical and numerical results* " International Journal of Rock Mechanics and Mining Sciences, vol. 41, pp. 245-253, 2004.

[2] Q. Z. Wang, L. Xing: "*Determination of fracture toughness KIC by using the flattended Brazilian disk specimen for rocks*", Engineering Fracture Mechanics, vol. 64, pp. 193{201, 1999.

[3] C. Keles, L. Tutluoglu: "*Investigation of proper specimen geometry for mode I fracture toughness testing with flattened Brazilian disc method* ", Int J Fract, 2011.

[4] D. H. Andersen, Z. L. Zhang: "*Fracture and physical properties of carbon anodes for the aluminum reduction cell*", Engineering Fracture Mechanics 78 (2011) 2998–3016

[5] A. A. Sharo: "*Pressure meter applications in laterally loaded drilled shaft socketed into transversely isotropic rock*", University of Akron, Ph. D, December 2009

[6] W. Wittke: "*Rock Mechanics Theory and Applications with Case Histories*" Spring-Verlag, Berlin Heidelberg, 1990

[7] T. L. Anderson: "*Fracture mechanics: Fundamentals and applications*", CRC Press, 2005.

[8] H. Liebowitz: "*Fracture: An Advanced Treatise*" , Volume II, Academic Press 1968

[9] R. C. Perruchoud, M W. Meier, W K. Fischer: "*Survey on worldwide prebaked anode quality*", Ligth Metals 2004

[8] If a 2-directional loading program is chosen, the anisotropy ratio $\frac{E^{\perp}}{E^{\parallel}}$ is disabled for user inputs since the program itself finds the ratio by the implemented equations.